Journal of Coastal Research	26	5	817–830	West Palm Beach, Florida	September 2010

Analyzing Estuarine Shoreline Change: A Case Study of Cedar Island, North Carolina

Lisa Cowart[†], J.P. Walsh[†‡]*, and D. Reide Corbett[†‡]

[†]Department of Geological Sciences
East Carolina University
Greenville, NC 27858, U.S.A.

[‡]Institute for Coastal Science and Policy
East Carolina University
Greenville, NC 27858, U.S.A.
walshj@ecu.edu

www.cerf-jcr.org

ABSTRACT

COWART, L.; WALSH, J.P., and CORBETT, D.R., 2010. Analyzing estuarine shoreline change: a case study of Cedar Island, North Carolina. *Journal of Coastal Research,* 26(5), 817–830. West Palm Beach (Florida), ISSN 0749-0208.

Continued climate change, sea-level rise, and coastal development have lead to concern about shoreline dynamics beyond oceanfront areas, encompassing more sheltered coastal water bodies such as estuaries. Because estuaries are critically important ecosystems, understanding coastline changes in these areas is necessary to evaluating resource risks. A transect-based approach is commonly used to quantify shoreline change on linear (*i.e.*, ocean) shorelines; however, due to the complex morphology of the study area, a point-based approach was developed and applied in this study. Shoreline-change rates and additional parameters (*i.e.*, wave energy and shoreline composition) were determined using 1958 and 1998 aerial photography and available datasets. From this data, the average shoreline change in the study area is -0.24 m yr^{-1}, with 88% of the shoreline eroding. Of the parameters analyzed, shoreline composition appears to have an important control on shoreline erosion, whereas wave energy is not significantly correlated with shoreline-change rates.

ADDITIONAL INDEX WORDS: *Erosion, fetch, shoreline composition, endpoint rate, transect.*

INTRODUCTION

Coastal erosion has been analyzed extensively along ocean shorelines, but more recent attention has focused on the movements and mechanisms of estuarine shoreline change (Benoit *et al.*, 2007). Sheltered from energetic open-ocean processes, estuaries are complex systems, enduring storms and offering a place of refuge for many organisms. Estuaries are biologically rich, productive ecosystems that are important for fish and shellfish growth and associated fisheries; approximately 75% of fish caught in the United States use estuaries during at least one stage in their lifetime (Martin *et al.*, 1996). Estuarine shorelines also act as natural buffers, diminishing the physical energy from waves and currents. Shorelines show great variability, accreting and eroding at different rates; this is evident in research performed by Riggs and Ames (2003), who measured considerable variations in erosion rates (0 to -7.6 m yr^{-1}) for shoreline types in eastern North Carolina.

The objective of this study is to analyze estuarine shoreline change at a high resolution (<100 m) over a large area to better understand how rates of shoreline change vary along Cedar Island and how this variation relates to the controlling processes. A new point-based approach was created to facilitate the effort and was applied to shorelines digitized from 1958 and 1998 imagery. Previous research (Price, 2006) used points to calculate shoreline change by pairing points located on each digitized shoreline spaced the same distance along the shoreline. However, the point-based approach created for this analysis calculated shoreline-change rates (SCRs) differently, using the closest linear distance between shorelines. The newly created point-based approach therefore calculates a conservative rate of shoreline change. Points were also used to analyze shoreline change for this study because of the ease with which additional parameters hypothesized to be important in estuarine erosion can be determined and analyzed. Parameters that reflect wave energy and shoreline composition are calculated from the shoreline points. These parameters are statistically analyzed to evaluate whether wave energy (using fetch and a wave exposure index as proxies) and shoreline composition (using elevation and vegetation as proxies) are critical controls on shoreline change along Cedar Island, North Carolina (Figure 1). The long-term shoreline-change results from the new point-based approach, based on digitized shorelines from 1958 and 1998, are compared with results from a commonly used transect-based approach.

Processes Affecting Shoreline Change

Recent media focus on climate change has drawn attention to sea-level rise and its potentially adverse affects on coastal systems (Dean, 2009). The physical effects of sea-level rise can include shoreline erosion, marine submergence, and inundation of low-lying coastal areas, and these effects may be magnified by increased storm events (Barth and Titus, 1984; Titus, 1990). Rising sea level is expected to widen and deepen estuaries as they are submerged and eroded (Bird, 1995). These changes are evident in Jamaica Bay, New York, where Hartig

DOI: 10.2112/JCOASTRES-D-09-00117.1 received 21 August 2009; accepted in revision 31 December 2009.

* Corresponding author.

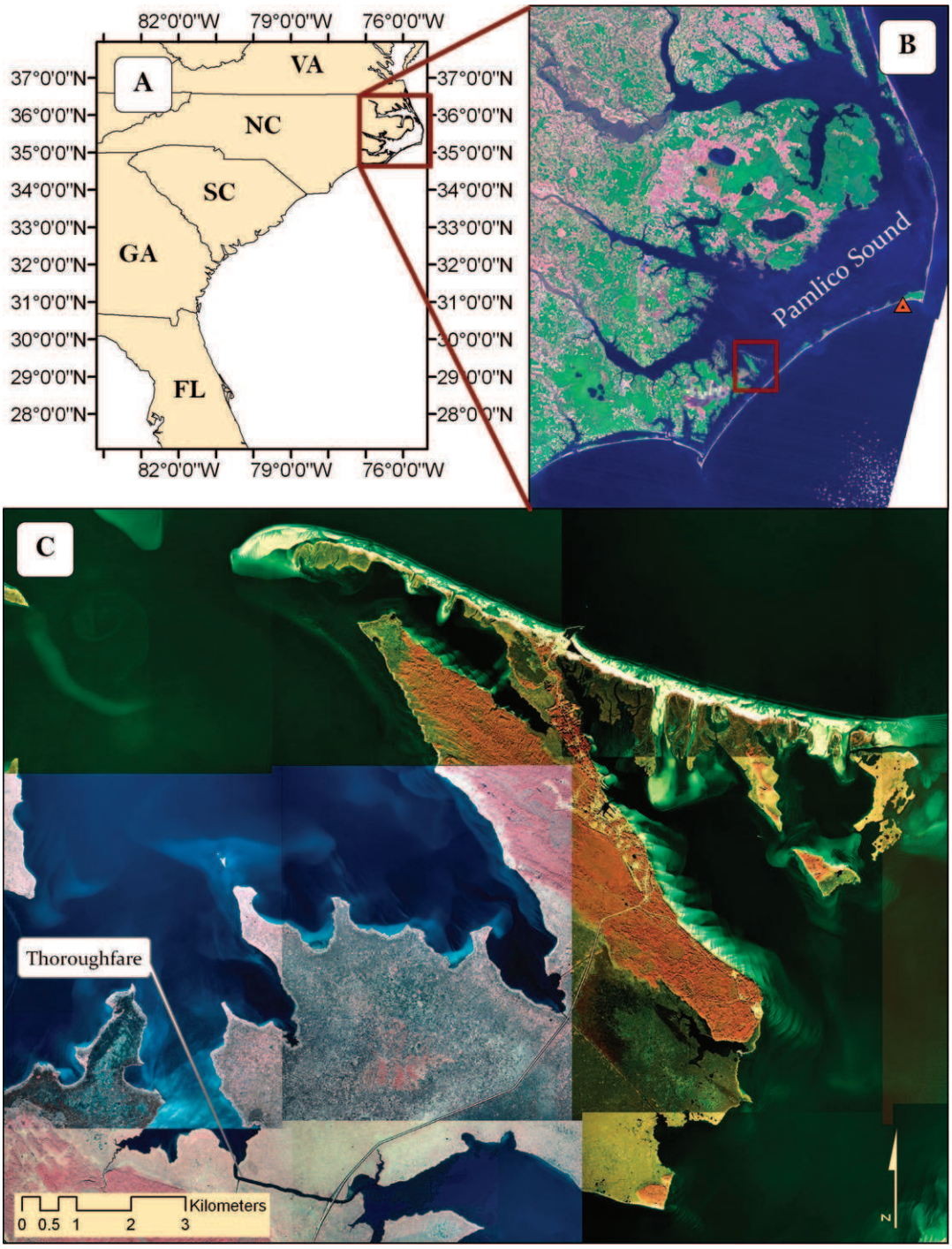

Figure 1. Location maps for the study area, including (A) the Albemarle–Pamlico Estuarine System, (B) the Cedar Island study area (red square) with the KHSE weather station location (closed triangle), and (C) the Cedar Island study area with 1998 digital orthophoto quarter quadrangles used in shoreline digitization. A color version of this figure is available in the online journal.

et al. (2002) document a 12% loss in marsh area over a 39-year period (1959 to 1998) in which local sea level rose 10.5 cm.

Although sea-level rise is one important factor affecting coastal erosion, other processes are expected to contribute, such as winds, waves, currents, bioerosion, and anthropogenic influences (Davis and Fitzgerald, 2004). Waves impacting the shoreline can suspend sediment, while currents can transport these materials elsewhere, causing erosion. Wave energy is a product of wind, bathymetry, and fetch. Erosion potential is higher in areas with larger fetches due to greater anticipated

wave buildup (Phillips, 1985). Waves impacting the shoreline are influenced by many factors, including shoreline elevation and vegetation. For example, Moller (2006) determined density and type of marsh vegetation were significantly related to wave height dissipation. While marshes are able to vertically accrete when flooded through sediment deposition, shorelines with elevations above sea level are expected to accrete more slowly, and depending on their size and lithology, these areas may experience mass wasting when acted upon by high-energy waves. For example, Phillips (1999) found that repeated storm events caused slope failure and recession on unconsolidated shoreline bluffs with relief of at least 1.5 m, while less shoreline retreat occurred on areas of lower elevation (*e.g.*, marsh, cypress fringe, and low-relief banks).

Calculating Shoreline Change

Shoreline change can be calculated through the time-series comparison of various data, including ground surveys, National Ocean Service topographic sheets, aerial photography, satellite imagery, synthetic aperture radar, light detection and ranging (LIDAR), and global positioning systems. Although new satellite and other remotely sensed approaches are becoming feasible (*e.g.*, LIDAR; Li, Di, and Ma, 2001), aerial photography analysis remains the most commonly used method to calculate shoreline change (Boak and Turner, 2005).

Due to the complex physical processes creating and moving sediments within the shore zone, spatial and temporal errors are potentially created when using aerial photography to calculate shoreline change. Spatial distortion is present in aerial photographs in the form of tilt, radial distortion, and relief displacement (see Crowell, Leatherman, and Buckley, 1991; Moore, 2000; and references therein). However, these distortions are generally corrected when the image is rectified. Rectification gives the image a spatial reference and is necessary before shoreline delineation. Temporal shoreline error exists because an aerial photograph is a snapshot in time of a dynamic system. For example, an image taken after a storm may display a shoreline that has retreated but has not yet recovered, and large storms can rapidly erode the shoreline, taking more than a year to recover (Douglas, Crowell, and Leatherman, 1998). However, through analyzing shoreline change in excess of a century, Fenster, Dolan, and Morton (2001) determined that storm-influenced data values are not outliers. Despite these inherent errors, Crowell, Leatherman, and Buckley (1991) determined a "worst-case error estimate" of 7.7 m using non-tide-coordinated aerial photography and geomorphic control, which exceeds the National Map Accuracy Standards (±12.2 m; U.S. Geological Survey [USGS], 1999).

Shoreline change can be calculated through various methods, including endpoint rate (EPR), average of rates, linear regression, and jackknifing, as discussed by Dolan, Fenster, and Holme (1991). The EPR is the most commonly used method due to its computational ease and because only two shorelines are required (Dolan, Fenster, and Holme, 1991). The EPR is calculated by measuring the distance between the shorelines and dividing by the time difference between the shorelines.

Analysis of shoreline change has often been conducted using an automated transect-based approach. In this approach, transects are created perpendicular to a baseline that is positioned landward or seaward of the shorelines being analyzed (Forbes *et al.*, 2004; Morton, Miller, and Moore, 2005; Thieler and Danforth, 1994a; Thieler, O'Connell, and Schupp, 2001). An EPR is calculated from the distance between shorelines along these fixed transects. The Digital Shoreline Analysis System (DSAS), created by and available from the USGS (Thieler and Danforth, 1994b), is a commonly used tool for transect-based shoreline-change analysis.

STUDY AREA

Cedar Island is located in Carteret County (34°57′ N, 76°22′ W), approximately 64 km northeast of Beaufort, North Carolina (Figure 1). It is part of the Albemarle–Pamlico Estuarine System (APES), the second-largest estuary in the United States, and is considered 1 of 28 "nationally significant" estuaries (Martin *et al.*, 1996). Cedar Island encompasses 58.6 km^2, with 44.5 km^2 consisting of flooded brackish marsh (Freske, 2007). Brinson, Bryant, and Jones (1991) describe three vegetation zones on Cedar Island; at the shoreline is zone 1, which consists primarily of *Juncus roemerianus* and *Distichlis spicata*, with the later being less abundant. In terms of physical energy, the shoreline of Cedar Island varies dramatically, from sheltered areas contained within the Thoroughfare, a canal separating the island from the mainland, to areas exposed to the vast fetches of Pamlico Sound and, thus, vulnerable to wave action. Cedar Island is sheltered from ocean processes and is dominated by wind waves and wind tides because the inlets of the Outer Banks chain of barrier islands restrict the flow of open-ocean waves and water into the estuarine system. Astronomical tides in the area are less than 10 cm (Benninger and Wells, 1993).

METHODS

Shoreline-Change Rates

To calculate SCRs in this study, 1998 digital orthophoto quarter quadrangles (DOQQs) and 1958 black-and-white aerial photographs were used; the methodological steps are illustrated in Figure 2. The 1998 DOQQs (1 × 1 m ground spatial resolution, in NAD 1983 State Plane NC FIPS 3200 projection) were obtained from the USGS in digital format. The 1958 aerial photographs were obtained from the North Carolina Geological Survey but were originally collected by Aerial Park Surveys, Inc., for the U.S. Department of Agriculture Commodity Stabilization Service. The 23 × 23 cm (9 × 9 inch) positive contact prints of the 1958 photographs were scanned using a Microtek ScanMaker 9800XL at 8-bit pixel resolution with a 600-dpi image resolution and were saved in TIFF format. Once in digital form, the 1958 photographs were rectified using the 1998 DOQQs and the georeferencing tools within ArcGIS®. Using the second-order polynomial transformation, the photographs were rectified with a minimum of eight ground control points. For the Cedar Island study area, 26 aerial photographs from 1958 were rectified with an average root-mean-square error of 1.68 m.

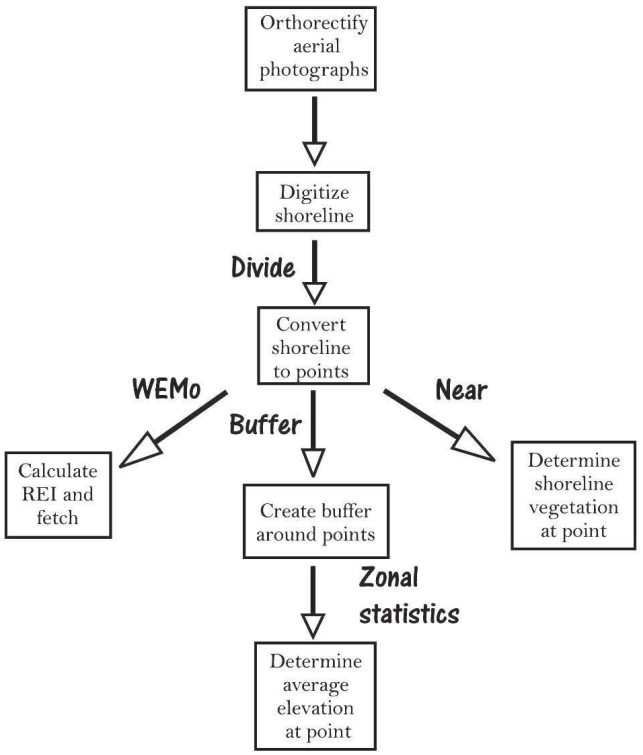

Figure 2. Flowchart of steps used to calculate parameters in this study. The methodology is derived from a combination of ArcGIS, wave exposure model, and Hawth's Tools.

Once aerial photographs were rectified, the wet–dry line was delineated on sediment shorelines (see Boak and Turner, 2005, and sources therein), whereas the apparent shoreline was digitized on vegetated shorelines (*i.e.*, the vegetation boundary; Ellis, 1978). The shorelines were digitized on-screen as a polyline using a zoom tolerance of 1 : 3500 to 1 : 3000 (Poulter, 2005). After digitization, a point was created every 50 m along the 1998 shoreline using the ArcGIS DIVIDE function (within the Editor toolbar), and the points were saved as a point shapefile. The EPR method was used to calculate the SCR at each point. The distances from the 1998 shoreline points to the 1958 shoreline were determined using the NEAR tool in ArcGIS (available with an ArcInfo license). The distance value was then divided by 40 years to calculate the SCR over the four-decade period between photographs. A polygon shapefile was generated from the 1958 shoreline polyline to define the initial land area. By intersecting the 1998 shoreline points with the 1958 polygon land area, the shoreline points that had moved landward were identified, *i.e.*, indicating erosion or negative shoreline change. The points that intersected the 1958 polygon were populated with a negative SCR value. The SCR of points that did not intersect the 1958 polygon—those that had accreted or where no shoreline change had occurred—remained positive. Because the nearest distance is used to calculate SCRs, the point-based approach determines conservative shoreline-change values. An example of the SCR methodology is shown in Figure 3 for a subset area from the study area. Shoreline recession occurred on the headland shorelines and the embayed shoreline; between, the headlands accreted.

The total positional uncertainty (U_T) of the shorelines and SCRs determined within this study were calculated based on work performed by Genz *et al.* (2007) and Fletcher *et al.* (2003). Of the error variables used by Genz *et al.* (2007) and Fletcher *et al.* (2003), three were used to calculate U_T for this study: the digitization error of the 1998 shoreline (E_{d1}), the digitization error of the 1958 shoreline (E_{d2}), and the rectification error (E_r):

$$U_T \pm \sqrt{E_{d1}^2 + E_{d2}^2 + E_r^2}$$

For shoreline-change analysis using aerial photography, the tidal fluctuation error can be incorporated; however, since the tidal fluctuation within the study area is minimal, this variable was not included in the positional uncertainty analysis. Through multiple digitization of the same area, a digitization error of 0.55 m was calculated for the 1998 and the 1958 shorelines. As stated previously, the 1958 rectified aerials had a root-mean-square error of 1.68 m; therefore, the U_T of the shorelines and SCR data is $\pm$1.85 m, or 0.05 m yr^{-1} over the 40-year period.

The calculated SCRs based on the point-based approach developed for this study were compared to values obtained through the more common transect-based approach using the DSAS program, version 3.0 (Thieler *et al.*, 2005). Within DSAS, SCRs were calculated along transects extending from baselines at multiple distances from the 1998 shoreline. Baselines were created by buffering the 1998 shoreline and then converting the polygon buffer to a polyline. The polyline was then clipped, and the landward portion of the line was used as the baseline.

Controlling Parameters

Several parameters identified in previous studies considered to affect estuarine erosion were determined at the 1998 shoreline points, including those reflecting wave energy and shoreline composition. To represent wave energy, a relative exposure index (REI) and fetch were calculated using a wave exposure model (WEMo). The WEMo is an ArcGIS tool developed by and available from the National Oceanic and Atmospheric Administration (NOAA) and has been used as a measure of wave exposure in submerged aquatic vegetation research (Fonseca *et al.*, 2002; see Malhotra and Fonseca, 2007, for a detailed description of WEMo). This numerical model calculates an REI, using directional wind speed, frequency of wind, fetch data, and bathymetry, to evaluate how exposed a site is to wind-generated waves in comparison to any other site. In WEMo, fetch is determined by radiating 32 lines at 11.25° angle increments from the point of interest. The fetch lines are then clipped to the area occupied by the bathymetric dataset to obtain the fetch length. To create a single representative metric of fetch, the 32 fetch lengths are averaged, producing the "mean fetch" value at each shoreline point. Fetch, bathymetry, and wind data are used to calculate the REI, a unitless value representing relative exposure. Bathymetry data is extracted from the NOAA Topographic Digital Elevation Model (TDEM) created from North Carolina Federal Emergency Management Agency LIDAR data, Shuttle Radar Topographic Mission data,

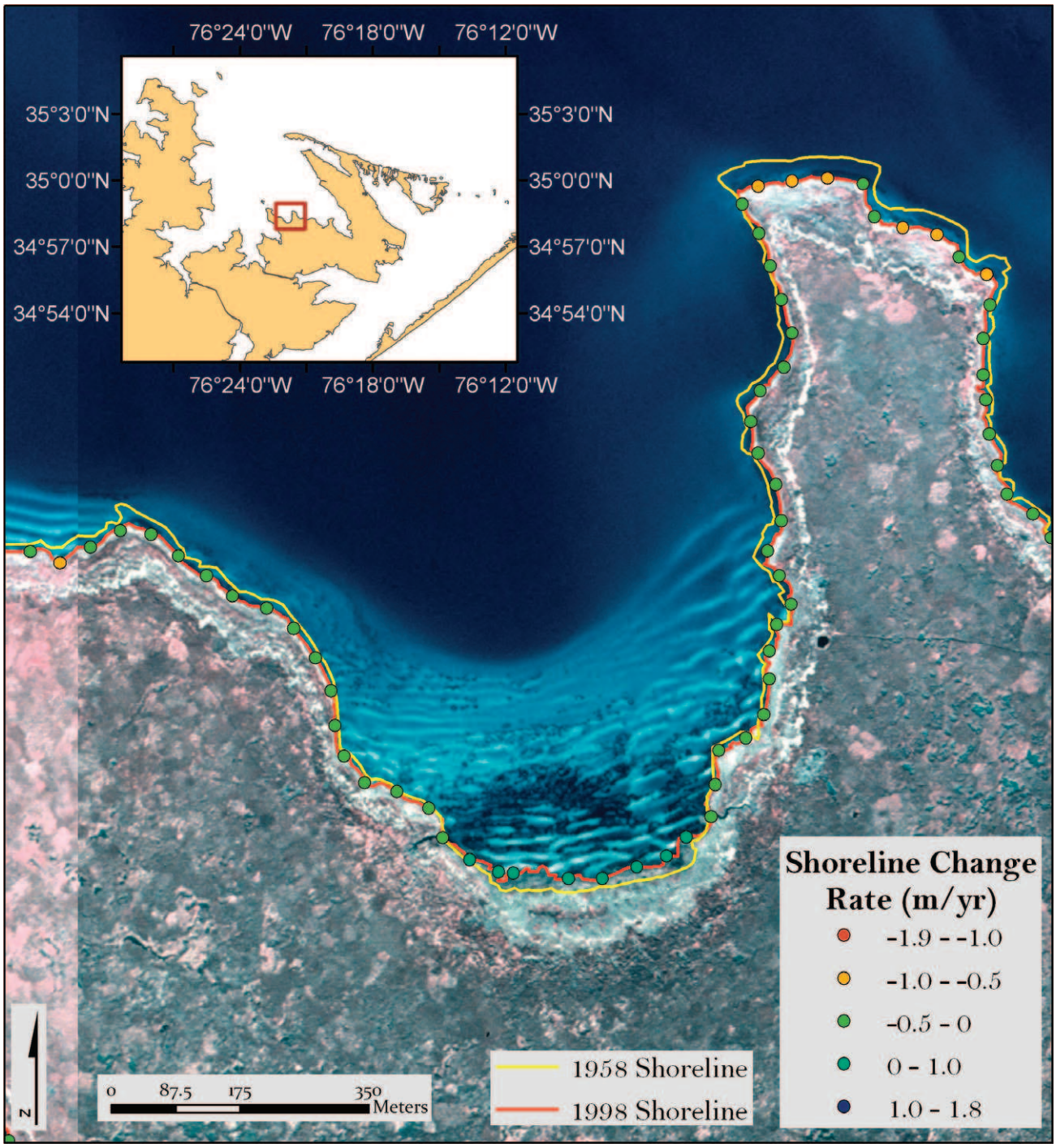

Figure 3. Shoreline-change rate (SCR) methodological summary displayed for a subset of the Cedar Island study area. The digitized shorelines from 1998 (red line) and 1958 (yellow line) are displayed. The SCRs are represented by distinctly colored points (see legend) derived using the point-based approach. Note the eroding shoreline on the headland and the accreting embayed area. A color version of this figure is available in the online journal.

the USGS Digital National Elevation Dataset, National Ocean Service sounding data, U.S. Army Corps of Engineers sounding data, Coastal Relief Model data, and digitized NOAA paper nautical charts (Hess *et al.*, 2004). The NOAA TDEM has a 6-m horizontal resolution and 20-cm vertical accuracy (North American Vertical Datum 88). Values less than zero were masked, using the ArcGIS spatial analyst extension, to create a raster dataset of values below sea level. Hourly wind data was

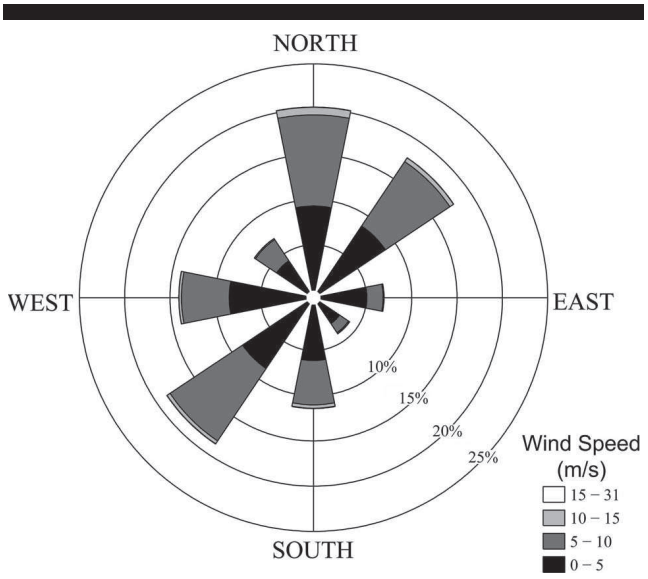

Figure 4. Rose diagram of wind data collected from the KHSE weather station (see Figure 1 for location). The plot is created from hourly wind data collected from 1958 to 1998.

obtained from the KHSE weather station, located in Hatteras, North Carolina (35°14′ N, 75°37′ W; Figure 1), for the four-decade period (1958–1998). From the wind data, average wind speeds and durations were calculated for the eight major compass-heading directions (Figure 4).

Shoreline composition was evaluated by determining the elevation and vegetation at the shoreline points. Shoreline elevation in this study is the elevation of the area surrounding each shoreline point and was determined using the topographic data within the NOAA TDEM. Elevation values greater than zero were masked, using the ArcGIS spatial analyst extension, to generate a raster dataset of land elevation values. The elevation at each point was assigned by determining the average value within a 25-m buffered area using zonal statistics within Hawth's Tools© (Beyer, 2007). Vegetation is a categorical variable that was determined using the 1997 NOAA land-use land-cover (LULC) dataset. This dataset consists of portions of three Landsat Thematic Mapper scenes analyzed according to the Coastal Change Analysis Program (C-CAP) protocol to determine land cover and subsequent change detection (Dobson *et al.*, 1995). The pixel resolution of the dataset is 30 m. Categories are high-intensity developed, low-intensity developed, cultivated land, grassland, deciduous forest, evergreen forest, mixed forest, scrub/shrub, palustrine forested wetland, palustrine scrub/shrub wetland, palustrine emergent wetland, estuarine forested wetland, estuarine scrub/shrub wetland, estuarine emergent wetland, unconsolidated shore, and bare land. Because shoreline points did not perfectly overlie the LULC data, the nearest value was associated with each shoreline point. This was accomplished by converting the LULC raster dataset to a point shapefile and then using the NEAR tool to determine the LULC type at each shoreline point.

RESULTS

Shoreline-Change Rates

Using the point-based approach, the SCR of the study area ranged from −1.89 to 1.74 m yr^{-1} and had an average of −0.24 m yr^{-1}, with 88% eroding, 2% showing no change (SCR = 0 m yr^{-1}), and 10% accreting (Table 1 and Figure 5A). As shown in the histogram within Figure 6, the SCR distribution was negatively skewed (skewness = −0.96), with 78% of the points clustering between 0 and −0.5 m yr^{-1}. Locations with greater erosion rates (more negative SCRs) occurred in the higher fetch areas on the northeast side of Cedar Island and on headland areas, whereas higher SCRs (less erosion and accretion) were located in embayed, sheltered areas (Figures 5A and D).

Using the transect-based approach (DSAS version 3.0; Thieler *et al.*, 2005), SCRs were calculated and varied depending on the baseline distance used (Table 2). For a 50-m baseline, the SCRs ranged from −6.9 m yr^{-1} to 1.2 m yr^{-1} with an average of −0.4 m yr^{-1}. The average SCR using a 200-m-baseline distance was similar (−0.4 m yr^{-1}), but the range was larger (39.5 m yr^{-1}) than that determined using a 50-m baseline distance (8.1 m yr^{-1}).

Wave Energy

Comparing the fetch values of the shoreline points for the eight major compass-heading directions (N, NE, E, SE, S, SW,

Table 1. *Descriptive statistics of parameters measured using the point-based approach (N = 1567). Mean fetch is calculated from averaging 32 fetch lengths.*

Parameter	Minimum	Maximum	Mean	Standard Deviation	Skewness	Kurtosis
Shoreline-change rate (m yr^{-1})	−1.89	1.74	−0.24	0.3	−1.0	5.8
Elevation (m)	0.01	3.16	0.61	0.5	2.7	8.3
Fetch (m)						
East	0	11,010	1369	3000	2.0	2.9
Northeast	0	60,890	2601	10,000	5.0	23.0
North	0	38,700	1727	6000	5.3	27.8
Northwest	0	35,298	2723	7000	3.1	9.2
West	0	9040	1219	2000	2.2	3.3
Southwest	0	13,209	853	2000	4.2	20.3
South	0	58,162	1169	4000	11.0	136.3
Southeast	0	11,679	1267	3000	2.2	4.0
Mean fetch (m)	0	9285	1478	1000	1.1	1.2
Relative exposure index	0	8387	318	900	5.6	40.1

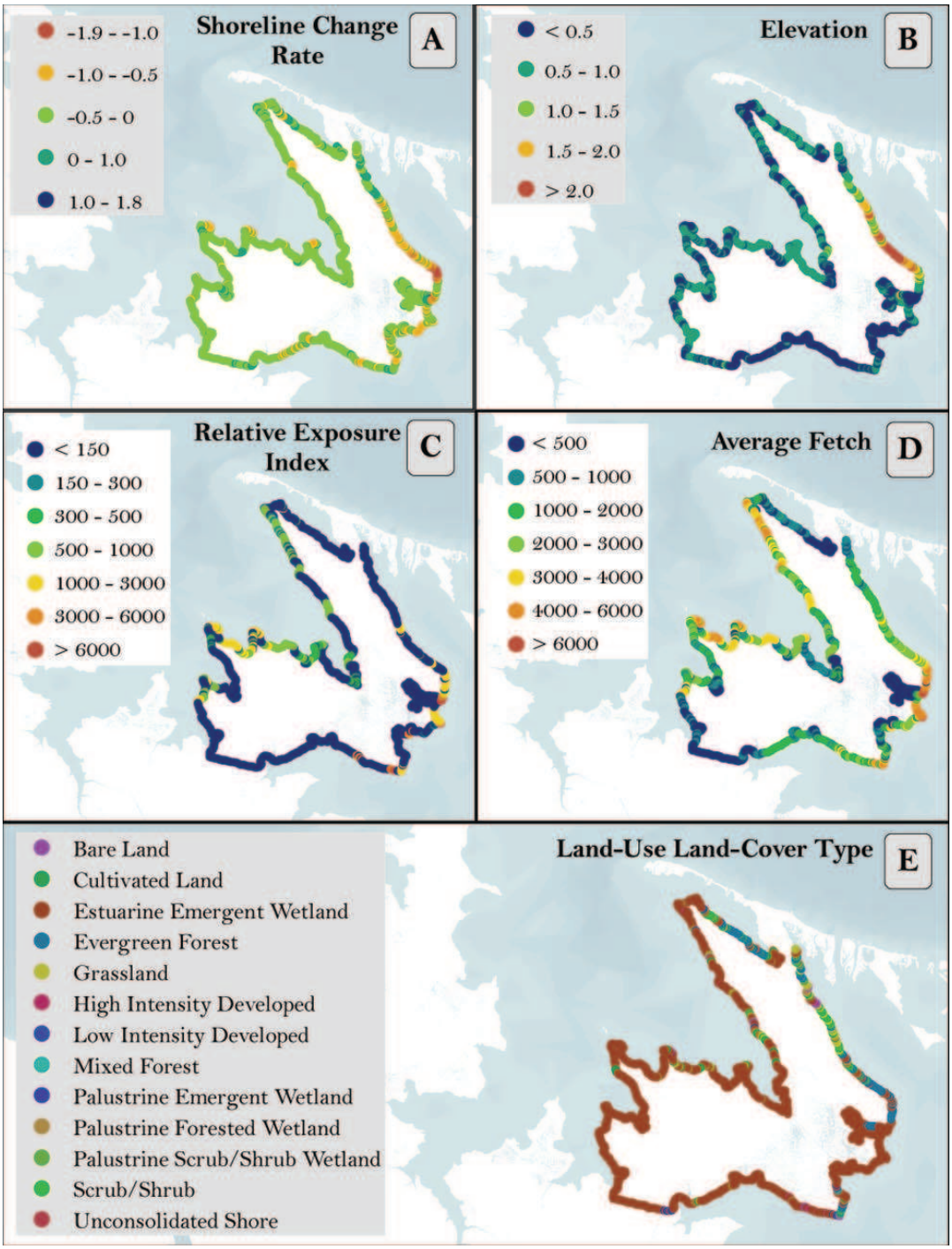

Figure 5. Maps of measured parameters: (A) shoreline-change rate (m yr^{-1}), (B) elevation (m), (C) relative exposure index, (D) average fetch (m), and (E) land-use land-cover type.

W, and NW), the mean northeastern and northern fetches were the largest while the mean western fetch was the lowest (Table 1). The "mean fetch" (average of 32 fetch lengths of the individual shoreline points) had a maximum value of 9285 m, with an overall average of 1478 m for the study area (Figure 5D and Table 1). The majority (95%) of the shoreline points with a mean fetch value greater than 1500 m were eroding. The REI values ranged from 0 to 8387, with an average of 318 (Table 1 and Figure 5C). Most shoreline points (95%) with an REI greater than the average (318) were eroding.

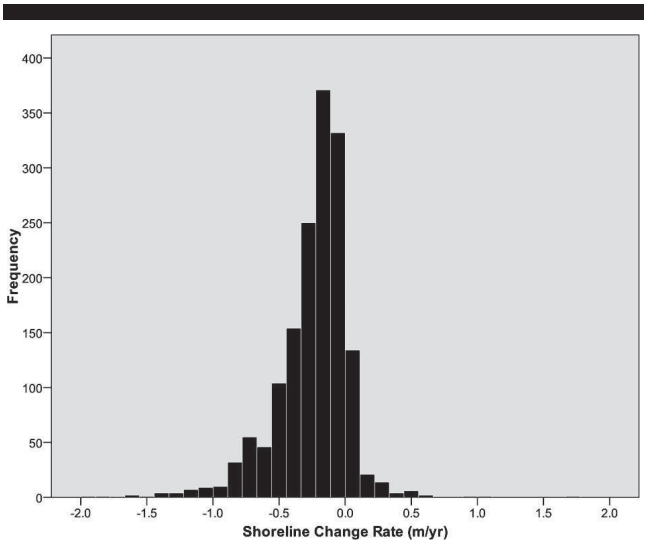

Figure 6. Histogram of shoreline-change rates (SCRs). The mean SCR of the 1567 points within the study area is -0.24 m yr^{-1}.

Shoreline Composition

The mean elevation of shoreline points in the study area was 0.6 m, with a range from 0 to 3.2 m. Half of the shoreline analyzed was at or below a 0.5-m elevation (Figure 5B), and the majority (90%) of the shoreline points were less than 1 m in elevation. Because the vertical accuracy of the elevation data is 20 cm, the elevation values were binned into 30-cm intervals and an analysis of variance (ANOVA) was performed to determine whether the mean SCRs located at higher elevation intervals were significantly different from the mean SCRs at lower elevation intervals (Figure 7). A Tukey test performed with 95% confidence in the ANOVA concluded that mean SCRs of elevation intervals greater than 1.2 m (mean SCRs < -0.60 m yr^{-1}) were significantly different from mean SCRs of elevation intervals lower than 1.2 m (mean SCRs $= -0.18$ to -0.26 m yr^{-1}).

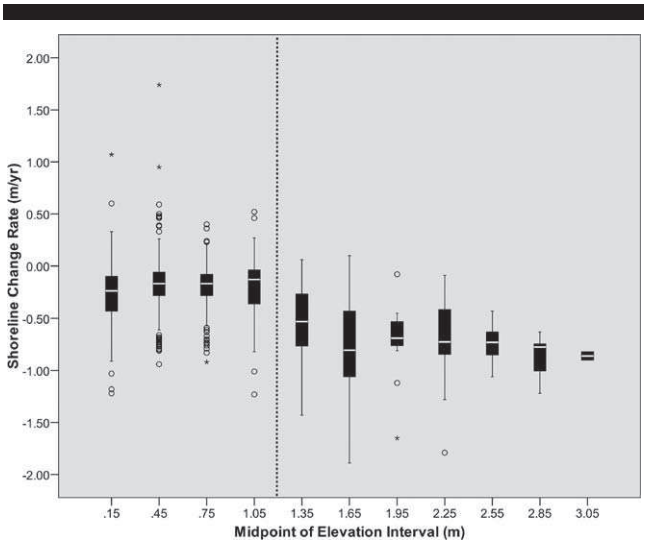

Figure 7. Box-and-whisker plot of elevation intervals and shoreline-change rates (SCRs) with the median value of the elevation interval on the x-axis. Outliers (open circles), extreme values (stars), and the median SCRs (white line within boxes) are displayed. The dotted line represents the 1.2-m elevation height on the x-axis.

Table 2. *Results using increasing baseline distances in the Digital Shoreline Analysis System with transects spaced 50 m apart.*

Baseline Distance (m)	Shoreline-Change Rate (m yr^{-1})				
	Minimum	Maximum	Mean	Median	Standard Deviation
25	−4.7	0.6	−0.3	−0.3	0.4
50	−6.9	1.2	−0.4	−0.3	0.5
150	−4.8	3.6	−0.4	−0.3	0.5
200	−36.3	3.2	−0.4	−0.3	1.6

Of the 16 LULC types within the C-CAP dataset, 13 types were present on the shoreline of the study area: bare land, cultivated land, estuarine emergent wetland, evergreen forest, grassland, high-intensity developed, low-intensity developed, mixed forest, palustrine emergent wetland, palustrine forested wetland, palustrine scrub/shrub wetland, scrub/shrub, and unconsolidated shore. The majority (79%) of the shoreline was composed of estuarine emergent wetland (Figures 5E and 8). Evergreen forest (7%) and scrub/shrub (5%) were the second and third most abundant LULC types, respectively. Together, the three LULC types covered 91% of the study area shoreline.

The average parameter values of the three most abundant LULC types are listed in Table 3. Using an ANOVA (Table 4), it was determined that the average SCR of the evergreen forest (-0.40 m yr^{-1}) and scrub/shrub (-0.39 m yr^{-1}) was significantly different from the average SCR of the estuarine emergent wetland (-0.22 m yr^{-1}) LULC type. A significant difference also was found between average elevations of the estuarine emergent wetland (0.51 m) and the evergreen forest (1.13 m) and scrub/shrub (1.09 m) LULC types. However, average fetch and REI values were not significantly different between LULC types.

DISCUSSION

Transect versus Point-Based Approach

Although the transect-based approach is commonly used to calculate shoreline change on ocean beaches and more sheltered coastlines (Morton, Miller, and Moore, 2005; Thieler and Danforth, 1994b; Thieler, O'Connell, and Schupp, 2001), some limitations occur when using it on highly sinuous shorelines. Transects generated using DSAS are also problematic when calculating SCRs along highly sinuous and headland shorelines (Figure 9). For example, Figure 9A displays a morphologically complex area that experienced both spit-growth accretion and shoreline erosion. In this area, the cuspate formation precludes the creation of the necessary transects to calculate shoreline movement. Highly sinuous areas are problematic using the transect method because transects are generated at varying angles from which highly oblique (*i.e.*, too large) SCRs are calculated. Figure 9B clearly

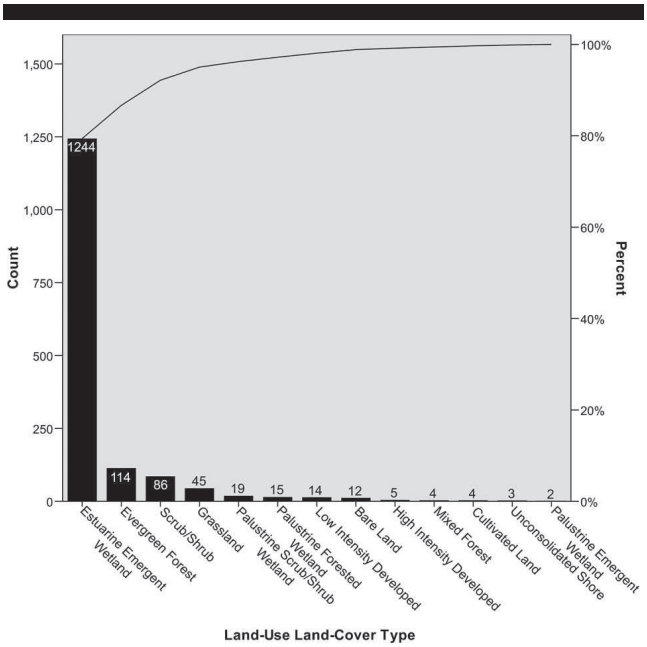

Figure 8. Histogram and cumulative frequency curve of land-use land-cover (LULC) types. The number of shoreline points is indicated in the white and black text corresponding to the bar for each LULC type. Estuarine emergent wetland is the dominant LULC, comprising 79% of the shoreline. The three most abundant LULC types (estuarine emergent wetland, evergreen forest, and scrub/shrub) compose 91% of the shoreline.

illustrates how transects spaced 50 m along the baseline have angles that overestimate the SCR values. It is also evident from our investigation that the distance of the baseline is critically important in calculating SCRs. Increasing the baseline distance decreases the number of transects created and therefore decreases the number (*i.e.*, resolution) of SCRs on headland areas, as shown in Figure 9C.

Other options are available when using DSAS to calculate SCRs, which include using an offshore or a straight baseline and creating smoothed transects. Creating an offshore or straight baseline may calculate accurate shoreline-change calculations on straight coastlines but would have problems

Table 3. *Summary of mean parameter values calculated for the three most abundant land-use land-cover (LULC) types. Through statistical analyses (analysis of variance and Tukey test), mean parameter values are determined to be significantly different where indicated.*

Parameter	Estuarine Emergent Wetland	Evergreen Forest	Scrub/ Shrub
Mean			
Shoreline-change rate (m yr^{-1})	−0.22*	−0.40†	−0.39†
Elevation (m)	0.51*	1.13†	1.10†
Fetch (m)	1407	1756	1737
Relative exposure index	334	243	200
Percentage of shoreline (%)	79	7	5

*Significantly different from the evergreen forest and scrub/shrub LULC types.
†Significantly different from the estuarine emergent wetland LULC type.

Table 4. *Summary of one-way analysis of variance for the three most abundant land-use land-cover (LULC) types (estuarine emergent wetland, evergreen forest, and scrub/shrub).*

Source of Variation	LULC df	LULC F-value
Shoreline-change rate	2	35.8†
Mean elevation	2	206.8†
Mean fetch	2	5.0*
Mean relative exposure index	2	1.5

*$P < 0.1$.
†$P < 0.01$.

similar to those previously discussed. The option of smoothed transects was not used within this study due to problems with software operation. Experienced users of DSAS may successfully employ this transect-based approach to calculate SCRs in complex areas; however, the trial-and-error process of determining the best application of the transect-based approach is time consuming and somewhat arbitrary. Therefore, the repeatability of the results may be limited.

Although the point-base approach is not yet an automated tool, it was found to be a simple, accurate, and efficient way to determine shoreline change over a large area at a high resolution. However, it is not without its limitations. Because the point-based approach determines SCRs using the nearest distance between shorelines, it is a conservative calculation of shoreline change. In addition, since the approach is not yet automated, it is manually executed. If shoreline change is being analyzed along a straight coastline, a transect-based approach may be more time efficient. However, as shown in this study, analysis of the estuarine shoreline benefits from a shoreline-change approach that is more sensitive to the sinuosity and morphologically complex areas, such as the point-base approach.

SCRs of Cedar Island, North Carolina

Previous work conducted on Cedar Island determined SCRs at 21 sites located 1 km apart from 1986 to 1987 and at 20 sites from 1987 through 1988 (Brinson, Bryant, and Jones, 1991). In this work, the average SCR from 1986 to 1987 was −0.47 m yr^{-1}, which is almost double the SCR determined in this study (−0.24 m yr^{-1}). However, the average SCR in this study was close to the SCR calculated by Brinson, Bryant, and Jones (1991) during the second year of analysis (−0.27 m yr^{-1}). Although these data have different spatial extent and resolution, the general agreement between the datasets is encouraging. The variation in the Brinson, Bryant, and Jones (1991) datasets may reflect the short-term variability in SCRs, and the similarity to the long-term rates calculated within this study suggests consistency at different timescales.

Through the analysis of 21 sites within the APES, SCRs were calculated by Riggs and Ames (2003); these sites were categorized into various shoreline types, including mainland marsh and low-sediment bank. The mainland marsh consisted of seven sites and had an average SCR of −0.91 m yr^{-1}, a considerably higher erosion rate than that determined for the estuarine emergent wetland shoreline (−0.22 m yr^{-1}) in this

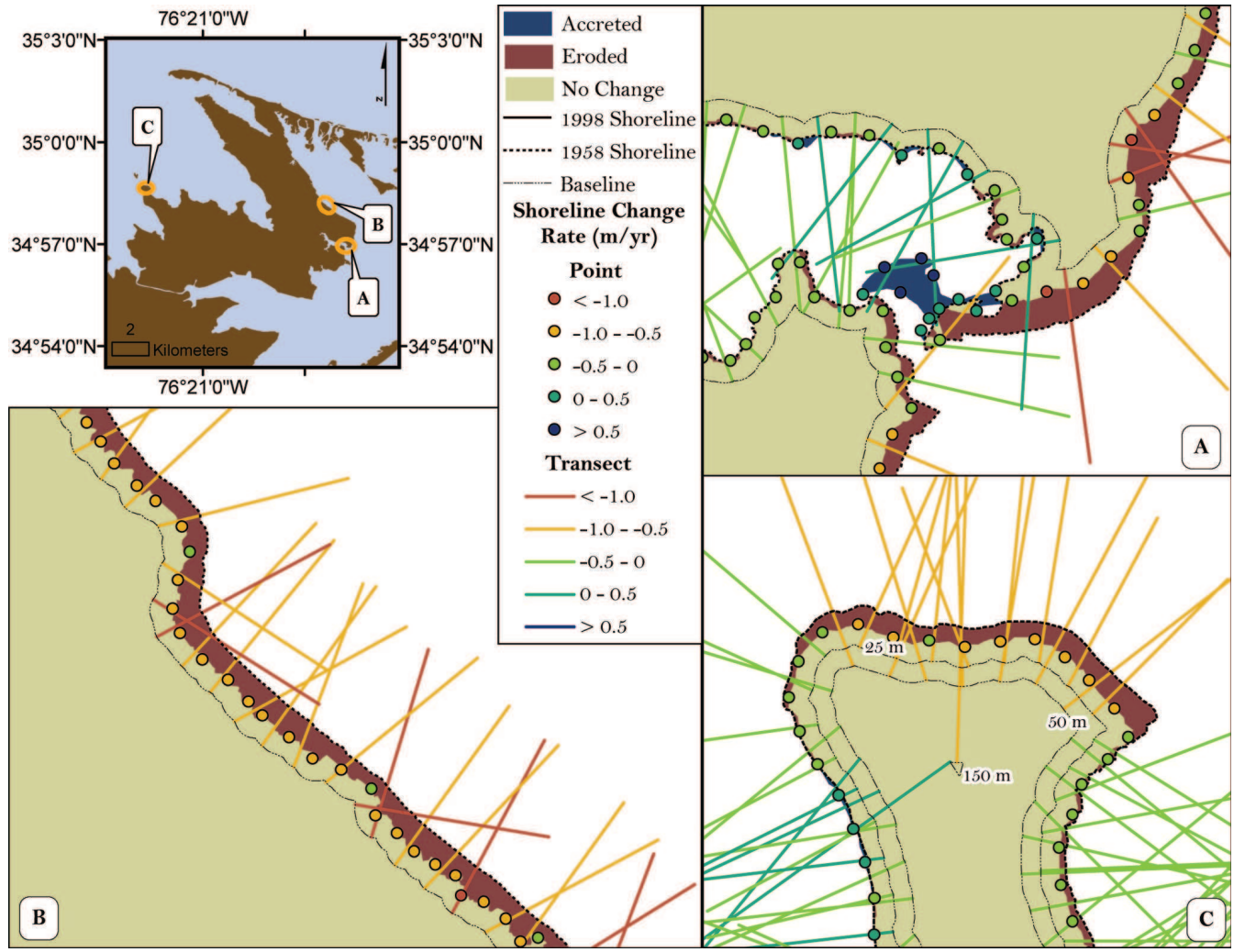

Figure 9. Location map and three subarea maps where the transect-based and the point-based approaches are compared. The shoreline area that has eroded, accreted, and not changed is represented as red, blue, and taupe, respectively. Shoreline-change rates (SCRs) are represented by transects and points using the same color scheme; therefore, in areas where transects and points do not have the same color, a different range of SCR is calculated. (A) The transect-based approach does not calculate shoreline change that occurred on the migrating spit. (B) Transects created perpendicular to the sinuous shoreline are at dramatic angles, therefore calculating SCRs larger than observed. (C) Baseline distance affects the SCRs calculated using the transect-based approach. As the baseline distance increases, the SCRs calculated decrease due to the decreased number of transects created.

study. However, considerable intersite variability in the average SCR was found within their study. For example, the northern side of Swan Quarter, which is described as more sheltered, *i.e.*, having low fetch, has a average SCR of (-0.37 m yr^{-1}), which is more comparable to our results. The higher rates observed in the APES study by Riggs and Ames (2003) were largely from sites that had been anthropogenically modified or experienced more exposed conditions; only a few sites were located in low fetch areas, which may explain the dramatic difference in mean rates. Also, the mainland marsh SCRs were measured over various periods, ranging from 14 to 42 years.

In comparison, similar average SCRs have been calculated on marshes in Rehoboth Bay, Delaware. Swisher (1982) determined an average SCR of -0.23 m yr^{-1} from aerial photography analysis from 1938 to 1981 on the southern shoreline of Horse Island, consisting of mainland marsh. On a shorter timescale (1995 to 1998), Schwimmer (2001) calculated an average SCR of -0.23 m yr^{-1} for the same area. Both short- and long-term SCR calculations are comparable to the average SCR for estuarine emergent wetland (-0.24 m yr^{-1}) calculated in this study.

Control of Wave Energy on SCRs

Wave energy is widely considered to be an important control on shoreline erosion rates. In previous work in Delaware Bay, wave energy flux, calculated from fetch, bathymetry, and wind data, was correlated with shoreline change (Schwimmer, 2001). To test the relationship between wave energy and SCR

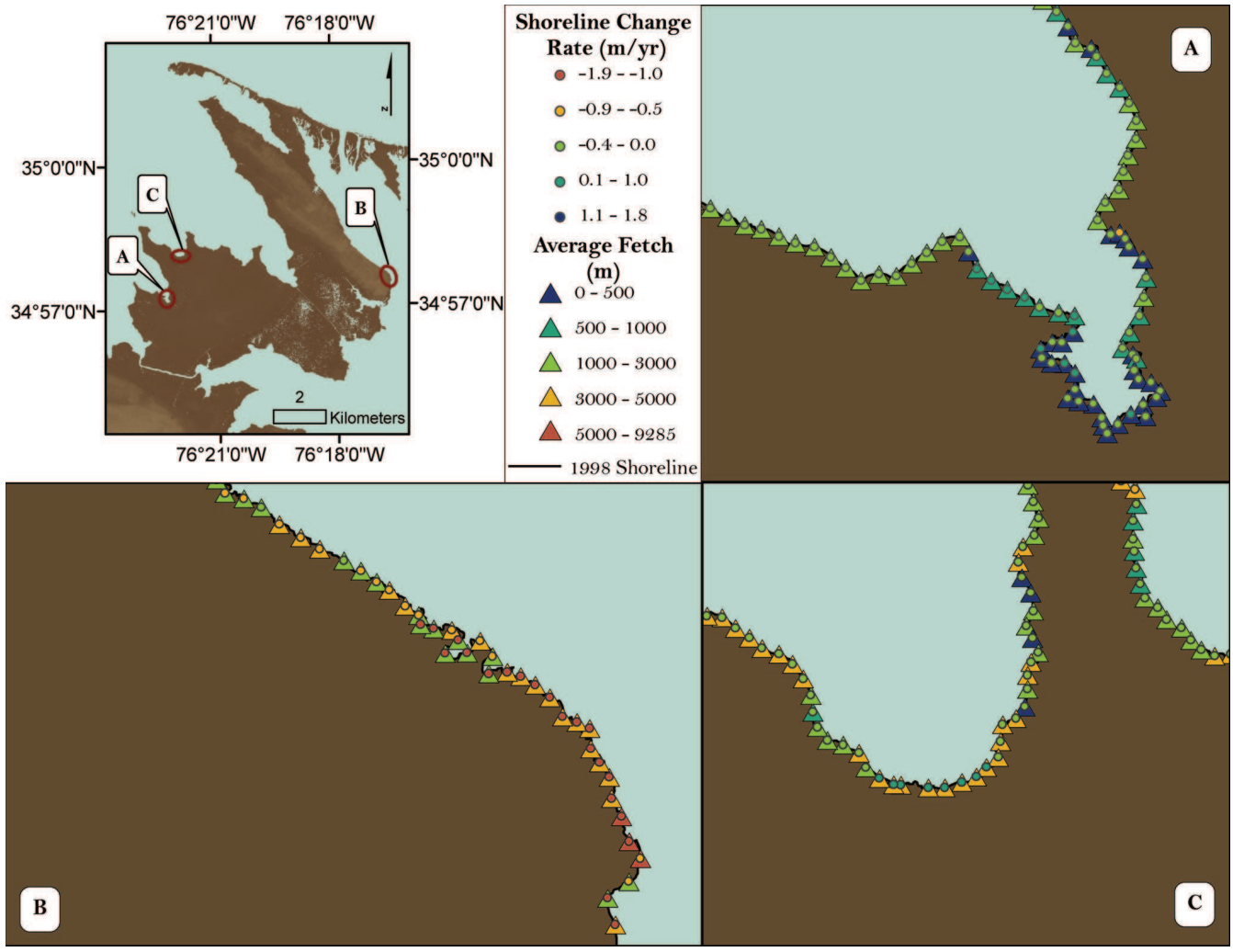

Figure 10. Location map and three subarea maps of mean fetch (triangles) and shoreline-change rate (SCR) values (circles). In some areas, mean fetch and SCRs exhibit the general relationship of (A) low mean fetch on shorelines with little to no erosion and (B) higher mean fetch on shorelines having higher erosion. However, these relationships were not observed throughout the study area. For example, (C) moderate-to-high mean fetch values occur on shorelines that are accreting.

along the shoreline, fetch and REI were measured to compare with SCRs. Qualitatively, in certain areas fetch and REI appear to have an obvious control. For example, headlands on the northern shore of the study area are found to have higher erosion than the embayed areas, lying between the headlands (Figure 5A). This pattern coincides with the general concept of wave refraction, where oncoming wave energy is focused on the headland area and the embayed area between headlands receives a reduced amount of wave energy in comparison.

Lower average fetch areas have higher SCRs (less erosive; Figure 10A), whereas higher average fetch values have higher erosion (more negative SCRs; Figure 10B). However, these patterns are not continuous throughout Cedar Island, as shown in Figure 10C, where an area of higher SCRs (little to no erosion) has high average fetch. When the collective dataset is analyzed, the statistical linear relationship between SCR and fetch and REI explained less than 15% of the variation in the data (Figure 11). Similarly, Brinson, Bryant, and Jones (1991) observed no apparent pattern between annual erosion rates (1986–1988) and fetch in the same study region. This may be attributed to the method of marsh erosion in the area, a function of undercutting softer sediments below the rhizosphere during low water, leading to slumping of the banks (Brinson, Bryant, and Jones, 1991; Knutson *et al.*, 1981). This occurs during low water driven by offshore winds. High water and waves created along the dominant fetch may be less erosive due to the armoring of marsh shorelines (Goodbred and Hine, 1995; Knutson *et al.*, 1982), leading to a lack of correlation between fetch and SCR.

Shoreline Composition Effects on SCRs

Data in this study indicate SCR may vary qualitatively with elevation of the coastline and among vegetation types,

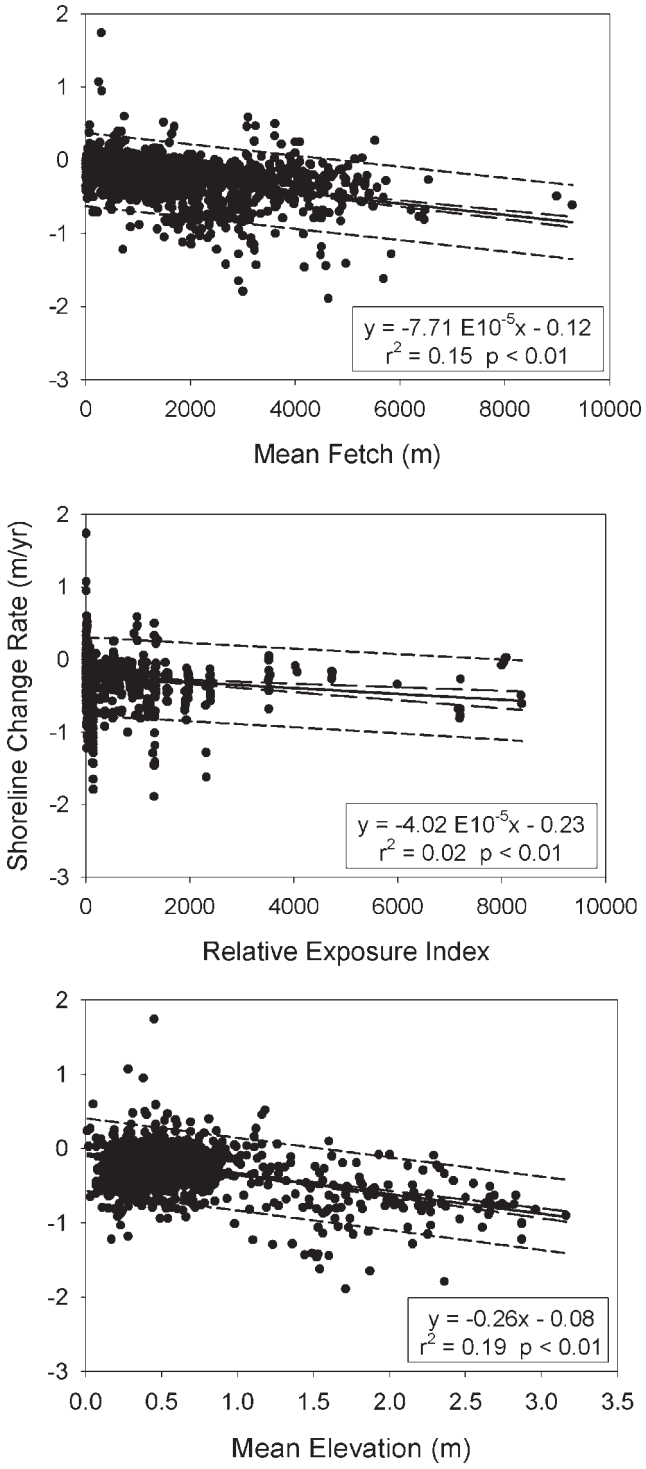

Figure 11. Linear relationship between shoreline-change rate and potential controlling parameters (mean fetch, relative exposure index, and mean elevation). A linear regression (solid line) has been applied, as well as the 95% confidence (long dashed) and prediction (short dashed) intervals. Note the low correlation coefficients for each parameter.

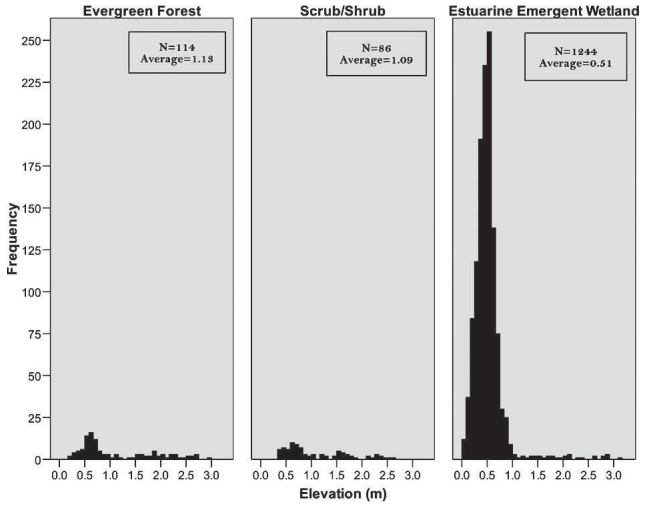

Figure 12. Histograms of elevation (m) for the three most abundant land-use land-cover (LULC) types (estuarine emergent wetland, evergreen forest, and scrub/shrub). The dominant LULC type (estuarine emergent wetland) has a lower mean elevation compared to the evergreen forest and scrub/shrub LULC types.

suggesting the importance of shoreline composition. Elevation intervals greater than 1.2 m have more negative average SCRs and are significantly different from average SCRs from areas with elevation intervals less than 1.2 m. However, like fetch and REI, the statistical linear relationship explained little (<20%) of the variation in the data (Figure 11) Among the three dominant LULC types (estuarine emergent wetland, evergreen forest, and scrub/shrub), the distribution of elevation shows a similar trend, where the lower-elevation LULC type (estuarine emergent wetland, 0.51 m) is significantly different from the higher-elevation LULC types (evergreen forest and scrub/shrub, each ~1 m) (Table 3 and Figure 12). These data suggest elevation, shoreline type, or both may be useful in predicting SCRs at these shoreline types.

The observed relationships between shoreline composition and SCRs are not surprising. It is known that marshes are difficult to erode due to their cohesive sediments, their binding roots, and the ability of marsh grass to accumulate sediments (Goodbred and Hine, 1995), aiding their ability to vertically accrete through sediment and organic matter accumulation (Craft, Seneca, and Broome, 1993; Nyman, Delaune, and Patrick, 1990; Nyman *et al.*, 2006). Recent work draws closer attention to shoreline composition (*i.e.*, bulk density, water content, percentage of organic matter, and grain size) as a primary control of lateral erosion rate (Feagin *et al.*, 2009). Riggs and Ames (2003) determine a higher SCR (less erosive) for marsh shorelines relative to low-sediment bank shorelines, which are nonmarsh areas with elevations of less than 1.5 m. Similarly, Riggs and Ames (2003) find low-sediment bank shorelines to have a relatively high SCR, comparable to our observations for evergreen forest and scrub/shrub. To summarize, the evergreen forest and scrub/shrub mean SCRs are more negative (more erosional) than the estuarine emergent wetland LULC type (Table 3). This relationship is similar to the SCRs

exhibited by the mainland marsh and low-sediment bank shorelines in Riggs and Ames (2003). Note, however, that the evergreen forest (-0.40 m yr^{-1}) and scrub/shrub (-0.39 m yr^{-1}) mean SCRs on Cedar Island (Table 3) are less negative (less erosional) compared to the low-sediment bank shorelines (-0.98 m yr^{-1}) analyzed by Riggs and Ames (2003). This may be related to different conditions (*e.g.*, water and nutrients), shoreline characteristics (*e.g.*, lithology or land use), or both. Further research is under way to explore statistical relationships over a larger area of coastal North Carolina. Through the present and previous studies, it is evident that a multiparameter approach is necessary to determine how estuarine shorelines change.

SUMMARY AND CONCLUSIONS

The development and management of coastal areas can benefit from the analysis of shoreline movement with time, including morphologically complex shorelines. A new point-based approach to calculate shoreline change at high resolution in sinuous and dynamic areas is presented and has been demonstrated to be effective. Using this methodology, the study area is shown to have an average SCR of -0.24 m yr^{-1} for the 40-year period analyzed (1958–1998). Based on the parameters analyzed, it is evident that shoreline composition (reflected by elevation and vegetation) appears to have an important control on SCRs, potentially more in this environment than wave energy (represented by fetch and a wave exposure index).

ACKNOWLEDGMENTS

Funding for this project was provided by the NOAA Coastal Ocean Program (NA05 NOS 4781182). The authors thank Dave Kunz, Jason Prior, Jeremy Brandsen, Haley Cleckner, Dorothea Ames, Amit Malhotra, and Tom Crawford for their contributions and assistance.

LITERATURE CITED

Barth, M.C. and Titus, J.G., 1984. *Greenhouse Effect and Sea Level Rise: A Challenge for This Generation*. New York: Van Nostrand Reinhold.

Benninger, L. K. and Wells, J. T., 1993. Sources of sediment to the Neuse River estuary, North Carolina. *Marine Chemistry*, 43, pp. 137–156.

Benoit, J.C.; Hardaway, C.S., Jr.; Hernansez, D.; Holman, R.; Koch, E.; McLellan, N.; Peterson, S.; Reed, D., and Suman, D., 2007. Mitigating Shore Erosion along Sheltered Coasts. National Research Council Division on Earth and Life Studies Ocean Studies Board. Washington, DC: National Academies Press.

Beyer, H.L., 2007. *Hawth's Analysis Tools for ArcGIS*, version 3.26. http://www.spatialecology.com (accessed May 21, 2007).

Bird, E.C., 1995. Present and future sea level: effects of predicted global changes. *In:* Eisma, D. (ed.), *Climate Change: Impact on Coastal Habitation*. Boca Raton, Florida: CRC Press, pp. 29–56.

Boak, E.H. and Turner, I.L., 2005. Shoreline definition and detection: a review. *Journal of Coastal Research*, 12, 688–703.

Brinson, M.M.; Bryant, W.L., and Jones, M.N., 1991. Composition, distribution and dynamics of organic sediments. *In:* Brinson, M.M. (ed.), *Ecology of a Nontidal Brackish Marsh in Coastal North Carolina*. Washington, DC: U.S. Fish and Wildlife Service and East Carolina University, pp. 23–46.

Craft, C.B.; Seneca, E.D., and Broome, S.W., 1993. Vertical accretion in microtidal regularly and irregularly flooded estuarine marshes. *Estuarine, Coastal and Shelf Science*, 37, 371–386.

Crowell, M.; Leatherman, S.P., and Buckley, M.K., 1991. Historical shoreline change: error analysis and mapping accuracy. *Journal of Coastal Research*, 7, 839–852.

Davis, R.A. and Fitzgerald, D.M., 2004. *Beaches and Coasts*. Malden, Massachusetts: Blackwell Publishing, 419p.

Dean, C., 2009. Sea's rise may prove the greater in Northeast. *The New York Times*, May 28, A15.

Dobson, J.E.; Bright, E.A.; Ferguson, R.L.; Field, D.W.; Wood, L.L.; Haddad, K.D.; Iredale, H., III; Jensen, J.R.; Klemas, V.V.; Orth, R.J., and Thomas, J.P., 1995. NOAA Coastal Change Analysis Program (C-CAP): Guidance for Regional Implementation. NOAA Technical Report NMFS 123. Seattle, Washington: Department of Commerce, 140p.

Dolan, R.; Fenster, M.S., and Holme, S.J., 1991. Temporal analysis of shoreline recession and accretion. *Journal of Coastal Research*, 7, 723–744.

Douglas, B.C.; Crowell, M., and Leatherman, S.P., 1998. Considerations for shoreline position prediction. *Journal of Coastal Research*, 14, 1025–1033.

Ellis, M.Y., 1978. *Coastal Mapping Handbook*. Department of the Interior, U.S. Geological Survey and U.S. Department of Commerce, National Ocean Service and Office of Coastal Zone Management. Washington, DC: U.S. Government Printing Office.

Feagin, R.A.; Lozada-Bernard, S.M.; Ravens, T.M.; Moller, I.; Yeager, K.M., and Baird, A.H., 2009. Does vegetation prevent wave erosion of salt marsh edges? *Proceedings of the National Academy of Sciences*, 106, 10109–10113.

Fenster, M.S.; Dolan, R., and Morton, R.A., 2001. Coastal storms and shoreline change: signal or noise? *Journal of Coastal Research*, 17, 714–720.

Fletcher, C.H.; Rooney, J.J.B.; Barbee, M.; Lim, S.-C., and Richmond, B.M., 2003. Mapping shoreline change using digital orthophotogrammetry on Maui, Hawaii. *Journal of Coastal Research*, Special Issue No. 38, pp. 106–124.

Fonseca, M.S.; Robbins, B.D.; Whitfield, P.E.; Wood, L., and Clinton, P., 2002. Evaluating the Effect of Offshore Sandbars on Seagrass Recovery and Restoration in Tampa Bay through Ecological Forecasting and Hindcasting of Exposure to Waves. St. Petersburg, Florida: Tampa Bay Estuary Program.

Forbes, D.L.; Parkes, G.S.; Manson, G.K., and Ketch, L.A., 2004. Storms and shoreline retreat in the southern Gulf of St. Lawrence. *Marine Geology*, 210, 169–204.

Freske, B., 2007. Cedar Island National Wildlife Refuge. U.S. Fish and Wildlife Service. http://www.fws.gov/southeast/pubs/facts/cdrcon.pdf (accessed September 11, 2007).

Genz, A.S.; Fletcher, C.H.; Dunn, R.A.; Frazer, L.N., and Rooney, J.J., 2007. The predictive accuracy of shoreline change rate methods and alongshore beach variation on Maui, Hawaii. *Journal of Coastal Research*, 23, 87–105.

Goodbred, S.L. and Hine, A.C., 1995. Coastal storm deposition: salt-marsh response to a severe extratropical storm, March 1993, west–central Florida. *Geology*, 23, 679–682.

Hartig, E.K.; Gornitz, V.; Kolker, A.; Mushacke, F., and Fallon, D., 2002 Anthropogenic and climate-change impacts on salt marshes of Jamaica Bay, New York City. *Wetlands*, 22, 71–89.

Hess, K.W.; White, S.A.; Sellars, J.; Spargo, E.A.; Wong, A.; Gill, S.K., and Zervas, C., 2004. North Carolina Sea Level Rise Project: Interim Technical Report. NOAA Technical Memorandum NOS CS 5. Silver Springs, Maryland: NOAA, 26p.

Knutson, P.L.; Brochu, R.A.; Seelig, W.N., and Inskeep, M., 1982. Wave damping in *Spartina alterniflora* marshes. *Wetlands*, 2, 87–104.

Knutson, P.L.; Ford, J.C.; Inskeep, M.R., and Oyler, J., 1981. National survey of planted salt marshes (vegetative stabilization and wave stress). *Wetlands*, 1, 129–157.

Li, R.; Di, K., and Ma, R., 2001. A comparative study on shoreline mapping techniques. The 4th International Symposium on Coastal GIS (Halifax, Nova Scotia, Canada), 11p.

Malhotra, A. and Fonseca, M.S., 2007. WEMo (Wave Exposure Model): Formulation, Procedures and Validation. NOAA Technical Memorandum NOS NCCOS 65. Beaufort, North Carolina: NOAA/

National Ocean Service/National Centers for Coastal Ocean Science, 28p.
Martin, D.M.; Morton, T.; Dobrzynski, T., and Valentine, B., 1996. *Estuaries on the Edge: The Vital Link between Land and Sea*. Washington, DC: American Oceans Campaign, 297p.
Moller, I., 2006. Quantifying saltmarsh vegetation and its effect on wave height dissipation: results from a UK east coast saltmarsh. *Estuarine, Coastal and Shelf Science*, 69, 337–351.
Moore, L.J., 2000. Shoreline mapping techniques. *Journal of Coastal Research*, 16, 111–124.
Morton, R.A.; Miller, T., and Moore, L., 2005. Historical shoreline changes along the U.S. Gulf of Mexico: a summary of recent shoreline comparisons and analyses. *Journal of Coastal Research*, 21, 704–709.
Nyman, J.A.; Delaune, R.D., and Patrick, W.H.J., 1990. Wetland soil formation in the rapidly subsiding Mississippi River deltaic plain: mineral and organic matter relationships. *Estuarine, Coastal and Shelf Science*, 31, 57–69.
Nyman, J.A.; Walters, R.J.; Deluane, R.D., and Patrick, W.H.J., 2006. Marsh vertical accretion *via* vegetative growth. *Estuarine, Coastal and Shelf Science*, 69, 370–380.
Phillips, J.D., 1985. Spatial Analysis of Shoreline Erosion, Delaware Bay, New Jersey. New Brunswick, New Jersey: Rutgers–The State University, Department of Geography, 194p.
Phillips, J.D., 1999. Event timing and sequence in coastal shoreline erosion: Hurricanes Bertha and Fran and the Neuse Estuary. *Journal of Coastal Research*, 15, 616–623.
Poulter, B., 2005. Interactions between Landscape Disturbances and Gradual Environmental Change: Plant Community Migration and Response to Fire and Sea-Level Rise. Durham, North Carolina: Duke University, Ph.D. dissertation, 216p.
Price, F.D., 2006. Quantification, Analysis, and Management of Intercoastal Waterway Channel Margin Erosion in the Guana Tolomato Matanzas National Estuarine Research Reserve, Florida. National Estuarine Research Reserve Technical Report Series 2006:1. http://www.nerrs.noaa.gov/Doc/PDF/Research/TechSeries200601.pdf (accessed May 20, 2007).
Riggs, S.R. and Ames, D.V., 2003. *Drowning the North Carolina Coast: Sea Level Rise and Estuarine Dynamics*. Raleigh: North Carolina Sea Grant, 152p.
Schwimmer, R.A., 2001. Rates and processes of marsh shoreline erosion in Rehoboth Bay, Delaware, U.S.A. *Journal of Coastal Research*, 17, 672–683.
Swisher, M.L., 1982. The Rates and Causes of Shore Erosion around a Transgressive Coastal Lagoon, Rehoboth Bay, Delaware, Newark: University of Delaware, College of Marine Studies, Master's thesis.
Thieler, E.R. and Danforth, W., 1994a. Historical shoreline mapping. I. Techniques and reducing positional errors. *Journal of Coastal Research*, 10, 549–563.
Thieler, E.R. and Danforth, W., 1994b. Historical shoreline mapping. II. Applications of the digital shoreline mapping and analysis systems (DSMS/DSAS) to shoreline change mapping in Puerto Rico. *Journal of Coastal Research*, 10, 600–620.
Thieler, E.R.; Himmelstoss, E.A.; Zichichi, J.L., and Miller, T.L., 2005. Digital Shoreline Analysis System (DSAS) version 3.0: An ArcGIS Extension for Calculating Shoreline Change. U.S. Geological Survey Open-File Report 2005-1304. http://woodshole.er.usgs.gov/project-pages/DSAS/version3/images/pdf/DSASv3_2.pdf (accessed May 22, 2007).
Thieler, E.R.; O'Connell, J.F., and Schupp, C.A., 2001. The Massachusetts Shoreline Change Project: 1800s to 1994. U.S. Geological Survey Administrative Report, http://www.mass.gov/czm/hazards/pdf/shorelinechangetechnicalreport.pdf (accessed May 27, 2007).
Titus, J.G., 1990. Greenhouse effect, sea level rise and land use. *Land Use Policy*, 7, 138–153.
United States Geological Survey, 1999. National Map Accuracy Standards. Fact Sheet FS-171-99. Reston, Virginia: U.S. Department of the Interior, USGS.